

LoRA-TTT: Low-Rank Test-Time Training for Vision-Language Models

Yuto Kojima Jiarui Xu Xueyan Zou Xiaolong Wang
UC San Diego

Abstract

The rapid advancements in vision-language models (VLMs), such as CLIP, have intensified the need to address distribution shifts between training and testing datasets. Although prior Test-Time Training (TTT) techniques for VLMs have demonstrated robust performance, they predominantly rely on tuning text prompts, a process that demands substantial computational resources and is heavily dependent on entropy-based loss. In this paper, we propose LoRA-TTT, a novel TTT method that leverages Low-Rank Adaptation (LoRA), applied exclusively to the image encoder of VLMs. By introducing LoRA and updating only its parameters during test time, our method offers a simple yet effective TTT approach, retaining the model’s initial generalization capability while achieving substantial performance gains with minimal memory and runtime overhead. Additionally, we introduce a highly efficient reconstruction loss tailored for TTT. Our method can adapt to diverse domains by combining these two losses, without increasing memory consumption or runtime. Extensive experiments on two benchmarks, covering 15 datasets, demonstrate that our method improves the zero-shot top-1 accuracy of CLIP-ViT-B/16 by an average of 5.79% on the OOD benchmark and 1.36% on the fine-grained benchmark, efficiently surpassing test-time prompt tuning, without relying on any external models or cache.

1. Introduction

Recent advancements in large-scale Vision-Language Models (VLMs) such as CLIP [44] and ALIGN [27] have enabled impressive zero-shot generalization across diverse tasks, leveraging extensive pre-training on noisy, web-scale image-text pairs [7, 46, 53]. However, VLMs often struggle to maintain robust performance under domain shifts [48, 62], a common challenge in real-world applications.

The original CLIP paper [44] has demonstrated that the choice of text prompts significantly impacts zero-shot image classification performance. As a result, the tedious work of pre-engineering text prompts for each downstream task has become increasingly important [5, 17, 76]. Ini-

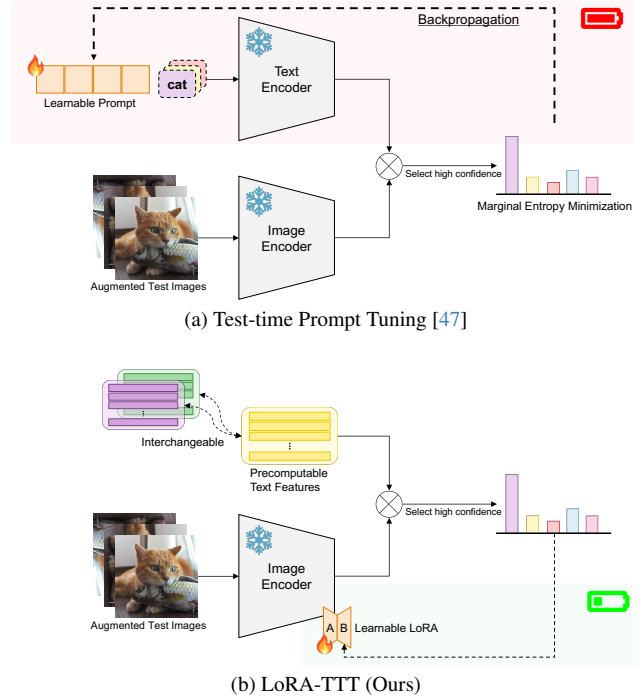


Figure S1. **Comparison of our proposed LoRA-TTT and Test-time Prompt Tuning (TPT).** (a) TPT optimizes the learnable text prompt via backpropagation, which results in high memory consumption, long runtime, and non-interchangeable text prompts. (b) LoRA-TTT requires only the image encoder and tunes only the LoRA parameters, demonstrating high performance while minimizing memory consumption and ensuring faster runtime. Additionally, it offers the flexibility of interchangeable text prompts.

tial works [74, 75] address the burden of prompt engineering by proposing prompt fine-tuning, which directly learns text prompts using a small amount of labeled data from the target domain. Recently, Test-Time Training (TTT) methods that adapt models during inference without requiring labeled data have gained significant attention [4, 8, 54]. Although several TTT methods for VLMs aimed at achieving zero-shot generalization have been proposed [39, 47, 51, 66], most rely on text prompt tuning, as it is simple, requires minimal modifications, and supports black-box adaptation—an advantage for VLMs with intellectual

property concerns [70]. However, text prompt tuning often requires intensive computation [28, 69], incurs high memory consumption, and offers limited flexibility in prompt selection [69]. For example, Fig. S1a illustrates TPT [47], a pioneering text prompt tuning method, where both the text encoder and image encoder are executed for each individual test instance, and the input text prompt — computationally intensive for backpropagation — is optimized from a fixed text prompt initialization during test time. In practice, TTT is frequently deployed in environments with memory-constrained edge devices [6, 49] and in scenarios requiring real-time data processing [2, 57] or flexible prompt combinations, highlighting the practical challenges of text prompt tuning.

The challenges of current TTT methods for VLMs lead to a simple question: *can we improve vision representation by directly tuning the image encoder, without relying on text prompt tuning, given that downstream tasks focus on vision tasks such as image classification, segmentation, and object detection?* Our hypothesis is that focusing on the image encoder can result in more effective and efficient adaptation in vision tasks. However, since VLMs are pre-trained on web-scale datasets, directly tuning the parameters of the image encoder on a test instance can degrade its generalization ability and lead to catastrophic forgetting [31, 60]. Inspired by recent advancements in Parameter Efficient Fine-Tuning (PEFT) [11, 19, 64] for large models, we propose a **Low-Rank Test-Time Training (LoRA-TTT)** that applies Low-Rank Adaptation (LoRA) [26] to the image encoder of VLMs. LoRA is proposed as one of the most extensively studied PEFT methods, effectively fine-tuning low-rank matrices connected in parallel to the fully connected matrices of each transformer layer, enabling the model to be tuned while preventing forgetting and minimizing memory consumption.

As shown in Fig. S1b, LoRA-TTT takes a novel approach from text prompt tuning by replacing the updated parameters from text prompts with LoRA parameters using entropy loss [47, 71]. Tuning only the LoRA parameters with a single instance during test time allows us to maintain a simple architecture and preserve the initial generalization ability, while adapting to the domain-specific features of the single instance. LoRA-TTT focuses exclusively on vision-side parameters, eliminating the need for the text encoder during test time by precomputing and storing text features. This reduces TTT runtime and significantly lowers memory consumption by avoiding memory-intensive text prompt tuning. The method also generalizes well to a wide range of text prompts without relying on specific prompt designs. In addition, focusing on the recent effectiveness of utilizing masked image modeling for TTT [15, 36, 57], we introduce a highly efficient reconstruction loss suited for TTT. This loss addresses the issue of overconfidence inherent in

entropy loss [18, 66], making it applicable in high-stakes environments [12, 29, 35, 58] where reliable model outputs are crucial. By combining the entropy and reconstruction loss, our method ensures zero-shot generalization across various domains and class categories without incurring computational overhead or additional memory consumption. Our contributions can be summarized as follows:

- We propose a **Low-Rank Test-Time Training (LoRA-TTT)**, which applies LoRA to the image encoder of VLMs. LoRA-TTT efficiently and effectively enhances zero-shot generalization capabilities without relying on teacher models or caching, making it well-suited for real-time processing on memory-constrained edge devices or in high-stakes environments.
- We introduce an efficient reconstruction loss suited for TTT, which can be combined with entropy loss. It demonstrates excellent calibration performance and can be easily adapted to real-world applications.
- We conduct comprehensive evaluations and comparisons with existing TTT techniques for VLMs across 15 datasets from two benchmarks, achieving state-of-the-art performance by simply replacing the text prompt with LoRA for the target parameters and combining two types of losses.

2. Related Work

Test-Time Training (TTT) allows models to adapt to distribution shifts between training and test data during inference through dynamic parameter updates [8, 34, 59]. The challenges in this area lie in designing an effective test-time objective without labels and developing an efficient system suitable for real-world deployment. For example, TENT [54] tunes batch normalization statistics at test time using entropy loss; however, this approach requires batch processing rather than instance-level processing, making it challenging to handle sequential data in real-time. Sun *et al.* [52] and Gandelsman *et al.* [15] update the image encoder by introducing auxiliary tasks and applying self-supervision; however, these methods require fine-tuning the model with auxiliary tasks beforehand for TTT. For VLMs, TPT [47] focuses on optimizing a text prompt at test time, valued for its simplicity and effectiveness. It demonstrates that augmenting a single test instance and calculating marginal entropy minimization [71] serves as an effective loss for VLMs. DiffTPT [14] utilizes stable diffusion to enhance data augmentation quality, while C-TPT [66] is a technique that calibrates TPT to improve reliability. RLCF [73] tunes the image encoder and demonstrates that CLIP-ViT-B can achieve performance comparable to CLIP-ViT-L but requires CLIP-ViT-L as a feedback source, which poses challenges in memory-constrained environments. Our method requires no external resources

and remains feasible even in closed memory-constrained environments such as edge devices.

Application of Low-rank adaptation (LoRA) aims to achieve efficient fine-tuning of large models with vast numbers of parameters in memory-constrained environments by introducing trainable low-rank matrices into each layer of the Transformer architecture, allowing the pre-trained parameters to remain frozen [19, 26, 63]. MeLo [77] demonstrates that applying LoRA to vision transformers (ViT) for downstream medical image diagnosis achieves comparable performance to fully fine-tuned ViT models while significantly reducing memory consumption. CLIP-LoRA [68] demonstrate significant performance improvements in few-shot learning by applying LoRA to the vision encoder of CLIP. However, CLIP-LoRA requires a few labeled samples from the target downstream task. To the best of our knowledge, no approach has applied LoRA for TTT in VLMs.

3. Method

3.1. Preliminaries

Contrastive Language-Image Pre-training (CLIP). Pre-training VLMs is typically conducted with specific vision-language objectives that facilitate learning image-text correspondences from extensive image and text datasets [44, 65, 67]. CLIP [44] consists of an image encoder g and a text encoder f , pre-trained using a contrastive loss to align the embeddings from both encoders in a shared feature space. After pre-training, CLIP exhibits strong zero-shot capabilities across various downstream tasks [32, 40, 44, 56]. For zero-shot image classification with CLIP, input text prompts are created by inserting each of the K -class category labels $\mathbb{Y} = y_1, y_2, \dots, y_K$ into a prompt prefix \mathbf{p} (e.g., $\mathbf{p}_i = \text{"a photo of a } y_i\text{"}$). The image X and the text input \mathbf{p}_i representing the i -th class are encoded into $\mathbf{v} = g(X)$ and $\mathbf{t}_i = f(\mathbf{p}_i)$ by their respective encoders. The classification score for the i -th class of image X is then calculated by

$$p(y_i | X) = \frac{\exp(\cos(\mathbf{t}_i \cdot \mathbf{v})/\tau)}{\sum_{i=1}^K \exp(\cos(\mathbf{t}_i \cdot \mathbf{v})/\tau)} \quad (1)$$

in zero-shot fashion, where τ is the temperature parameter and $\cos(\cdot, \cdot)$ represents the cosine similarity.

TPT [47] makes the text prompt prefix trainable $\mathbf{p} \in \mathbb{R}^{L \times D}$ instead of using pre-determined, hand-crafted prompt, where L represents the number of tokens and D is the embedding size of the text encoder. TPT optimizes the learnable text prompt using backpropagation with Marginal Entropy Minimization (MEM) loss [71] from each test instance. A test image instance undergoes data augmentation N times $\{X_n\}_{n=1}^N$, and the top N_p samples with the highest

confidence are selected to calculate the MEM loss, filtering out noisy augmented views. The entropy of the predicted probability distribution over the K -classes is calculated by

$$\mathcal{L}_{\text{MEM}} = - \sum_{i=1}^K \bar{p}(y_i | X) \log(\bar{p}(y_i | X)), \quad (2)$$

where $\bar{p}(\cdot | X) = \frac{1}{N_p} \sum_{n=1}^{N_p} p(\cdot | X_n)$. MEM loss has become the de facto standard in modern TTT for VLMs. [13].

LoRA [26] represents the incremental adjustment of pre-trained weights by injecting two small matrices, based on the concept of the intrinsic rank of downstream domain shifts [1]. Given that $\mathbf{W}_0 \in \mathbb{R}^{d_1 \times d_2}$ is a pre-trained weight matrix in the network, with \mathbf{x} as the input and \mathbf{h} as the hidden state, the forward pass after applying LoRA is given by:

$$\mathbf{h} = \mathbf{W}_0 \mathbf{x} + \Delta \mathbf{W} \mathbf{x} = \mathbf{W}_0 \mathbf{x} + \gamma \mathbf{B} \mathbf{A} \mathbf{x}, \quad (3)$$

where $\mathbf{A} \in \mathbb{R}^{r \times d_2}$ and $\mathbf{B} \in \mathbb{R}^{d_1 \times r}$ are the two small matrices introduced by LoRA. γ is a constant scale hyperparameter that determines the contribution of LoRA in the subsequent layers. The intrinsic rank r is typically much smaller than d_1 and d_2 . Therefore, by freezing the pre-trained matrix and updating only the parameters of the \mathbf{A} and \mathbf{B} matrices during fine-tuning, the number of parameters that need to be updated can be significantly reduced. In the original LoRA paper, LoRA is applied to the key, query, value, and output matrices on the attention matrices of transformer-based models.

3.2. LoRA-TTT

Application of LoRA for TTT. Focusing on the current mainstream method, TPT, our approach shifts the target of parameter updates from the text prompt to the image encoder, while leveraging the MEM loss. However, directly updating the entire image encoder is expected to result in excessive memory consumption and domain-specific behaviors that lose the out-of-distribution generalization and robustness of foundation models [31, 60]. As shown in Fig. S2, inspired by the effectiveness of LoRA in the large language model field, we apply LoRA to layers of the image encoder in VLMs, updating only the LoRA parameters during test time. The original LoRA paper shows that the change in weights during model adaptation has a low intrinsic rank and we hypothesize that LoRA can adapt to unique domain-specific features of each instance even with unlabeled data similar to fine-tuning in downstream tasks. By applying LoRA, we adjust only a small number of parameters without altering the original well pre-trained weights in VLMs. This approach allows individual adaptation to each test instance while preserving

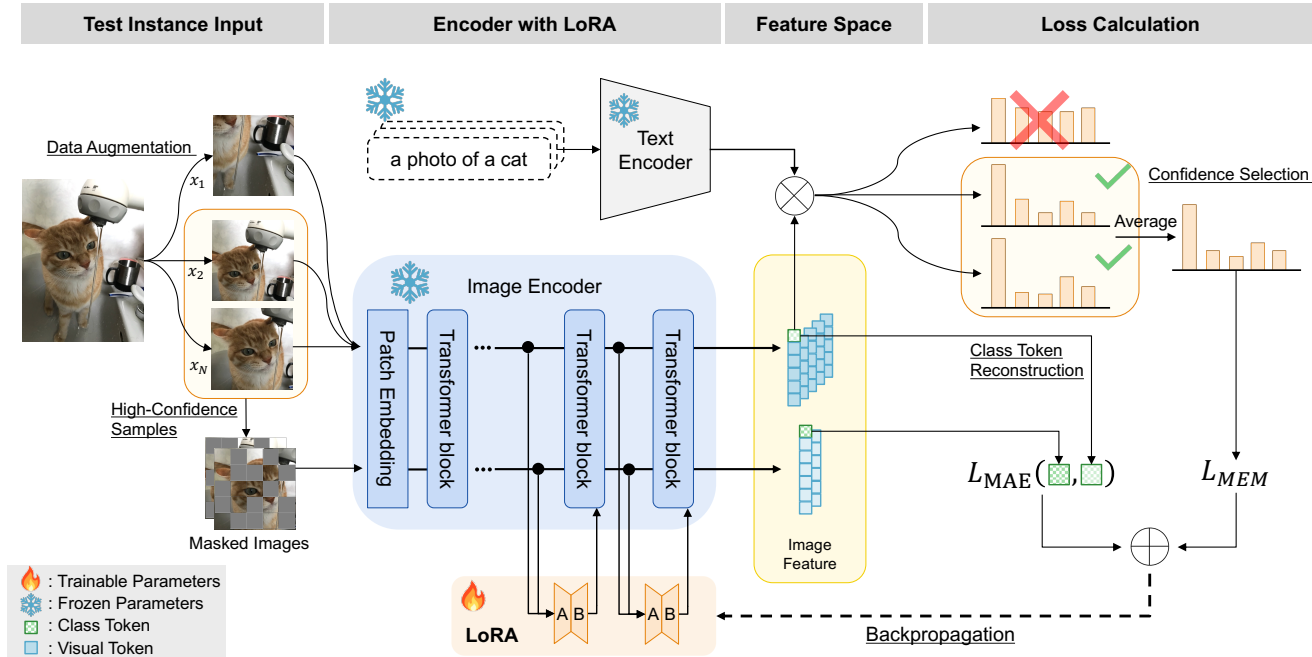


Figure S2. **LoRA-TTT** for zero-shot image classification. Our method applies LoRA to the layers of the image encoder in VLMs. LoRA-TTT updates the LoRA parameters using MEM loss and MAE loss, calculated from the top 10% of high-confidence augmented views. This approach allows adaptation to domain shifts with low memory consumption while maintaining generalization ability.

the strong zero-shot capability of the original VLMs and reducing memory consumption during backpropagation. Furthermore, LoRA-TTT applies LoRA exclusively to the vision encoder of VLMs, rendering the text encoder unnecessary during TTT. This allows the model to be tuned independently of specific text prompts. Following the approach of Episodic TTT [47, 54, 73], we update parameters using only a single test instance and reset them afterward, ensuring a certain level of robustness against sequence data.

Masked Image Reconstruction for VLMs. LoRA-TTT is not limited by the type of loss function. We are able to leverage a self-supervised reconstruction loss based on masked autoencoders (MAE) [15, 21], owing to the benefits of parameterizing the image encoder. LoRA-TTT differs from conventional TTT methods based on MAE [15, 57] and offers an efficient solution suitable for TTT, as it requires neither an image decoder nor fine-tuning of the model prior to TTT. LoRA-TTT takes both augmented images and their randomly masked versions as input to the image encoder and calculates the mean squared error of only the encoded class tokens as the loss. These images are selected from the top 10% of views with the highest confidence, similar to TPT. We optimize the following loss:

$$\mathcal{L}_{MAE} = \text{MSE}(g(X)_{\text{cls}}, g(\text{mask}(X))_{\text{cls}}), \quad (4)$$

where $\text{MSE}(\cdot, \cdot)$ represents the mean squared error between

the encoded class tokens of the masked and unmasked images, $\text{mask}()$ randomly masks out majority of the input image patches (e.g., 50%). This loss encourages the model to reconstruct the original global features by leveraging the remaining visual clues, enhancing visual understanding to better support downstream tasks. The total loss can be expressed as $\mathcal{L} = \lambda_1 \mathcal{L}_{MEM} + \lambda_2 \mathcal{L}_{MAE}$, where λ_1 and λ_2 are coefficients that balance the two losses.

4. Experiments

This section reports benchmark results for zero-shot image classification, comparing our proposed approach with previous methods. Following prior work [14, 28, 47], we evaluate out-of-distribution (OOD) performance on 4 datasets derived from ImageNet and fine-grained (FG) classification on 10 datasets spanning various categories.

4.1. Experimental setup

Datasets. For the OOD benchmark, we use ImageNet [10] and its variants including ImageNet-A [24], ImageNet-V2 [45], ImageNet-R [23], and ImageNet-Sketch [55], to evaluate robustness against 4 out-of-distribution patterns derived from ImageNet. Additionally, we evaluate 10 different datasets for the fine-grained benchmark. These datasets encompass a wide range of categories, including plants and animals (Flower102 [42], OxfordPets [43]), scene recognition (SUN397 [61]), textures (DTD [9]),

Table S1. **Top1 accuracy of zero-shot image classification on the OOD benchmark** when using the default hard prompt. The results of CoCoOp are obtained from the TPT paper, while others are reproduced with our code. The best results under zero-shot conditions are highlighted in **bold**. Performance improvements over the zero-shot CLIP-ViT-B/16 are indicated with an upward blue arrow (\uparrow blue) and a downward red arrow (\downarrow red).

Method	ImageNet	ImageNet-A	ImageNet-V2	ImageNet-R	ImageNet-Sketch	Average	OOD Avg.
CLIP-ViT-B/16	66.71	47.80	60.63	73.99	46.15	59.06	57.14
CoOp [75]	71.75	50.13	64.51	75.28	47.92	61.92	59.46
CoCoOp [74]	71.02	50.63	64.07	76.18	48.75	62.13	59.91
TPT [47]	69.02	54.73	63.70	77.15	47.99	62.52	60.89
C-TPT [66]	68.50	51.60	62.70	76.00	47.90	61.34	59.55
MTA [69]	69.23	56.87	63.67	76.88	48.54	63.04	61.49
Image Encoder Tuning	64.26	56.31	59.70	75.89	47.65	60.76	59.89
LoRA-TTT-M (Ours)	69.21(\uparrow 2.49)	60.57 (\uparrow 12.77)	64.28(\uparrow 3.65)	77.53(\uparrow 3.54)	48.73(\uparrow 2.57)	64.06(\uparrow 5.01)	62.78(\uparrow 5.64)
LoRA-TTT-A (Ours)	66.27(\downarrow 0.45)	52.55(\uparrow 4.75)	60.87(\uparrow 0.24)	75.57(\uparrow 1.58)	47.01(\uparrow 0.85)	60.45(\uparrow 1.39)	59.00(\uparrow 1.86)
LoRA-TTT (Ours)	69.40 (\uparrow 2.68)	60.52(\uparrow 12.72)	64.43 (\uparrow 3.80)	77.84 (\uparrow 3.85)	48.94 (\uparrow 2.79)	64.23 (\uparrow 5.17)	62.93 (\uparrow 5.79)

food (Food101 [3]), transportation (StanfordCars [30], Aircraft [38]), human actions (UCF101 [50]), satellite images (EuroSAT [22]), and general objects (Caltech101 [33]). This benchmark assesses the applicability of our TTT method across a diverse range of categories.

Baselines. We compare our method with the baseline CLIP-ViT-B/16 and few-shot learning methods — CoOp [75], CoCoOp [74] — as well as existing test-time prompt tuning methods — TPT [47] and C-TPT [66]. Additionally, we compare Image Encoder Tuning, which tunes the image encoder parameters without relying on LoRA, and MTA [69], which operates without backpropagation. For a fair comparison, we focus on methods that do not rely on external models or cached data.

Implementation details. We adopt the pre-trained CLIP-ViT-B/16 as the common backbone architecture. In text prompt tuning methods, the number of trainable text tokens is set to 4, with initial weights based on the prompt “a photo of a”. We prepare three versions as precomputed text prompts: the default hard prompt “a photo of a” to match the initialization commonly used in text prompt tuning, an ensemble of 80 different hand-crafted prompts [44], and CoOp [75]. The weights of CoOp are pre-trained on ImageNet with 16 shots and 4 tokens. LoRA is applied exclusively to the transformer architecture in layers 11 and 12 of the image encoder with a rank of 16 targeting the key, query, value, and output matrices. The LoRA scale γ is set to 12 for the OOD benchmark and 2 for the fine-grained benchmark. Matrix A of LoRA is initialized using Kaiming-uniform [20], while matrix B is initialized to zero. For the test-time loss variants of our method, **LoRA-TTT-M** uses the MEM loss only, **LoRA-TTT-A** uses the MAE loss only, and **LoRA-TTT** combines the two losses with the weights set to $\lambda_1 = 1$ and $\lambda_2 = 16$. We optimize the

LoRA parameters in a single step, using the AdamW optimizer [37] with a learning rate of 0.001 and a weight decay value of 0.2. For Image Encoder Tuning, we use the same optimizer and loss settings as in **LoRA-TTT** for a fair comparison, directly tuning the parameters of the key, query, value, and output matrices in the transformer layers 11 and 12 of the image encoder. Data augmentation follows TPT by expanding a single instance into a 64-batch using random resized crops, including the original instance. Additionally, the top 10% of high-confidence samples from the batch of 64 are selected to compute the test losses and filter out noisy views. All the experiments are conducted using a single NVIDIA RTX 3090 GPU with 24GB of memory.

4.2. Results

Zero-shot classification. In Tab. S1 and Tab. S2, LoRA-TTT enhances the zero-shot generalization capacity of CLIP-ViT-B/16, outperforming both few-shot learning and text prompt tuning methods on average across the two benchmark evaluations. Notably, it significantly surpasses existing methods on the OOD benchmark, demonstrating that it is a highly effective approach for adapting to various domains. LoRA-TTT achieves state-of-the-art performance among methods that do not rely on domain knowledge, additional models, or cache. Despite Image Encoder Tuning failing to adapt effectively to the fine-grained benchmark, LoRA-TTT consistently delivers significantly better results, showing improvements of 3.04% in OOD and 3.63% in fine-grained averages compared to Image Encoder Tuning. This confirms that LoRA tuning is effective for adapting to domain gaps in VLMs, helping to prevent forgetting and making it a suitable approach for TTT.

In the comparison of the two test-time losses, LoRA-TTT-M and LoRA-TTT-A, both methods show performance improvements over the baseline. In Tab. S2, LoRA-TTT-A (*i.e.*, MAE loss) achieves comparable or

Table S2. **Top-1 accuracy of zero-shot image classification on the fine-grained benchmark** using the default hard prompt. CoCoOp is from the TPT paper, while others are reproduced with our code. The best results under zero-shot conditions are in **bold**. Performance improvements over zero-shot CLIP-ViT-B/16 are indicated with an upward blue arrow (\uparrow blue) and a downward red arrow (\downarrow red).

Method	Flower102	DTD	Pets	Cars	UCF101	Caltech	Food101	SUN397	Aircraft	EuroSAT	FG Avg.
CLIP-ViT-B/16	67.40	44.39	88.25	65.51	65.24	93.31	83.64	62.56	23.91	42.22	63.64
CoOp [75]	68.30	42.34	89.35	63.30	67.19	92.85	83.72	64.53	19.96	40.19	63.17
CoCoOp [74]	70.85	45.45	90.46	64.90	68.44	93.79	83.97	66.89	22.29	39.23	64.63
TPT [47]	68.98	45.92	87.27	67.02	68.99	93.55	85.00	65.11	23.76	43.44	64.91
C-TPT [66]	69.67	44.80	88.47	65.97	65.27	93.35	83.23	64.28	23.97	42.21	64.12
MTA [69]	68.29	45.33	88.17	68.08	68.07	94.12	84.88	64.72	25.38	40.91	64.79
Image Encoder Tuning	59.03	42.91	83.81	66.60	67.57	88.64	82.11	62.71	23.67	36.67	61.37
LoRA-TTT-M (Ours)	67.60(\uparrow 0.20)	46.04 (\uparrow 1.65)	87.11(\downarrow 1.14)	67.81(\uparrow 2.30)	68.38(\uparrow 3.15)	93.59(\uparrow 0.28)	84.83(\uparrow 1.19)	64.61(\uparrow 2.05)	25.68(\uparrow 1.77)	39.27(\downarrow 2.95)	64.49(\uparrow 0.85)
LoRA-TTT-A (Ours)	68.33(\uparrow 0.93)	45.21(\uparrow 0.83)	88.72 (\uparrow 0.46)	66.94(\uparrow 1.43)	66.35(\uparrow 1.11)	93.71(\uparrow 0.41)	84.39(\uparrow 0.75)	63.63(\uparrow 1.07)	25.38(\uparrow 1.47)	44.52 (\uparrow 2.30)	64.72(\uparrow 1.08)
LoRA-TTT (Ours)	67.88(\uparrow 0.49)	45.80(\uparrow 1.48)	87.63(\downarrow 0.63)	67.72(\uparrow 2.20)	68.38(\uparrow 3.15)	93.83(\uparrow 0.53)	84.99(\uparrow 1.35)	64.59(\uparrow 2.03)	25.92 (\uparrow 2.01)	43.23(\uparrow 1.01)	65.00 (\uparrow 1.36)

Table S3. **Generalization in prompts.** Performance differences from each single hard prompt are indicated with an upward blue arrow (\uparrow blue) and a downward red arrow (\downarrow red).

Method	ImageNet	OOD Average	FG Average
CLIP-ViT-B/16 + Ensemble	68.31(\uparrow 1.59)	59.52(\uparrow 2.38)	64.68(\uparrow 1.04)
TPT + Ensemble	67.21(\downarrow 1.81)	59.93(\downarrow 0.96)	63.37(\downarrow 1.54)
LoRA-TTT+ Ensemble (Ours)	70.67 (\uparrow 1.27)	64.99 (\uparrow 2.06)	65.95 (\uparrow 0.95)
CLIP-ViT-B/16 + CoOp	71.75(\uparrow 5.03)	59.46(\uparrow 2.32)	63.17(\downarrow 0.47)
TPT + CoOp	73.63(\uparrow 4.62)	62.98(\uparrow 2.09)	63.95(\downarrow 0.95)
LoRA-TTT+ CoOp (Ours)	74.03 (\uparrow 4.63)	64.35 (\uparrow 1.42)	64.00 (\downarrow 1.01)

better results than LoRA-TTT-M (*i.e.*, MEM loss) across a wide range of category domains in the fine-grained benchmark, particularly demonstrating the high versatility of MAE as a test-time loss in VLMs. Although our use of MAE loss involves only an image encoder without a decoder, it demonstrates that restoring global features of masked images contributes to understanding image context in VLMs. Combining the two losses further enhances both versatility and performance, surpassing TPT in the fine-grained benchmark. For example, a comparison of TPT with LoRA-TTT-M on EuroSAT highlights the importance of tuning the text prompt when using only the MEM loss, but the combination with the MAE loss helps overcome this weakness.

Generalization in prompts. Tab. S3 shows the generalization performance when using either the ensemble of text prompts or CoOp. TPT is designed to initialize a single hard prompt, making it not straightforward to combine with the ensemble of prompts. In our implementation of TPT, we initialize the prompt using the average of embeddings from the text prompts. By combining our method with the ensemble, we achieve performance improvements comparable to those of CLIP-ViT-B/16 with the ensemble, significantly surpassing the state-of-the-art in text prompt tuning while maintaining zero-shot conditions. Even when combined with CoOp, a few-shot learning approach, LoRA-TTT shows a similar trend to CLIP-ViT-B/16 +

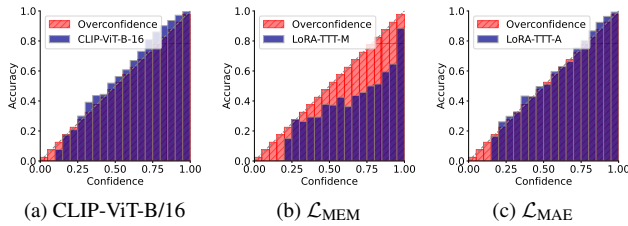
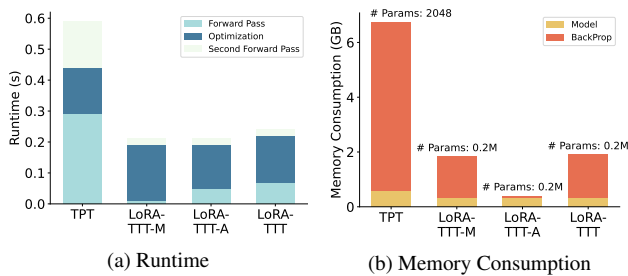
CoOp, indicating that our method improves performance independently of the text prompt. Our method focuses solely on tuning the parameters within the image encoder, allowing for greater flexibility in designing text prompts, an advantage in practical applications where the ability to freely choose prompts is beneficial [17].

Calibration. As shown in Fig. S3b, \mathcal{L}_{MEM} , commonly used as a test-time loss in VLMs, is known to induce overconfidence [18, 66], where the model’s predicted confidence exceeds its actual accuracy. Calibration is quantified using Expected Calibration Error (ECE) [41], which measures alignment between predicted probabilities and actual outcomes. Tab. S4 compares the ECE for our loss functions, TPT, and C-TPT. Since LoRA-TTT-A (*i.e.*, MAE loss) is not explicitly designed based on confidence, it retains its original calibration properties. LoRA-TTT-A achieves ECE performance comparable to or better than C-TPT, without any specific efforts for calibration, even though C-TPT is designed to improve the calibration performance of TPT. From a TTT perspective, the MAE loss demonstrates advantages not only in generalization across various domains but also in calibration, which is essential given the critical role of prediction uncertainty in real-world applications such as healthcare diagnostics [35, 58] and autonomous vehicles [12, 29].

Efficiency. Runtime and memory consumption, shown in Fig. S4a and Fig. S4b, demonstrate the efficiency of our approach compared to TPT. Our method precomputes text features and eliminates the need for a text encoder during TTT. This reduces model size and shortens forward pass times both before and after optimization compared to TPT where text encoding often serves as a bottleneck. Although LoRA-TTT has a substantially larger number of trainable parameters than TPT, it limits LoRA application to the deeper layers of the image encoder, reducing memory usage during backpropagation. Notably, LoRA-TTT-A significantly reduces memory usage during backpropa-

Table S4. **Expected Calibration Error** (\downarrow).

Method	ImageNet	OOD Average	FG Average
CLIP-ViT-B/16	1.93	4.80	4.53
TPT	10.61	12.08	11.71
C-TPT	3.11	5.38	5.29
LoRA-TTT-M	20.32	22.76	19.73
LoRA-TTT-A	2.97	5.59	4.80
LoRA-TTT	14.04	16.49	12.75

Figure S3. **Comparison of calibration performance on the Cars dataset.** The MAE loss can improve performance while preserving the baseline model’s output characteristics.Figure S4. **TTT efficiency in ImageNet evaluation.** The efficiency of TPT heavily depends on the number of classes and input text tokens. To optimize TPT, the number of tokens is set to 20, including the 4 learnable tokens, matching the length of the longest class name in the dataset.

gation, primarily by calculating the loss from only 10% of the augmented images and masking half of the tokens. Consequently, it requires minimal additional resources even when the MAE loss is included in the total loss. LoRA-TTT achieves higher efficiency than TPT while delivering significantly superior performance. Based on these results, LoRA-TTT is adaptable to a wide range of domains and applications, including streaming data processing [2, 57], from high-stakes environments [12, 29, 35, 58] to memory-constrained edge devices [6, 49].

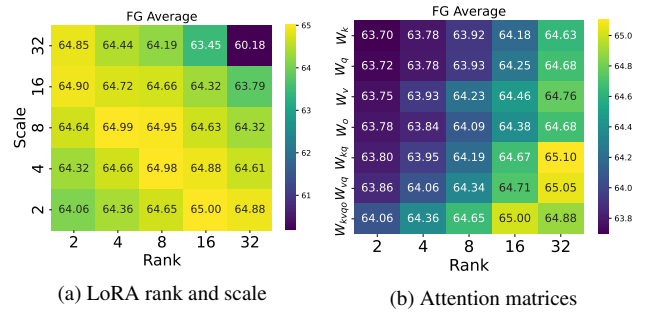
5. Ablation Study

5.1. How to apply LoRA for TTT

In this section, we explore the utilization of LoRA for TTT. We investigate the key factors for effectively applying LoRA, including: (1) determining the optimal layers and

Table S5. **Layers for LoRA application.**

LoRA Layer	ImageNet	OOD Average	FG Average
12	69.59	62.65	64.68
11-12	69.40	62.93	65.00
9-12	68.97	62.86	64.73
5-8	66.88	61.34	64.83
1-4	67.99	60.69	64.56
All	68.12	62.54	64.62

Figure S5. **Impact of LoRA application design.** The average top-1 accuracy on the fine-grained benchmark is shown, with LoRA applied to layers 11 and 12 of the image encoder.

the extent of LoRA application within the transformer model, (2) understanding the relationship between the appropriate rank and scale, and (3) selecting the attention matrices for tuning.

Which layers should we apply LoRA to?

Tab. S5 presents the zero-shot classification performance when LoRA is applied to specific layers of the image encoder in CLIP-ViT-B/16. Our results indicate that applying LoRA to deeper layers is more effective than to shallower ones, aligning with trends observed in fine-tuning language models [72]. Additionally, applying LoRA to more layers does not necessarily improve performance. Limiting its application to the 11th and 12th layers not only outperforms applying it across all layers in terms of performance but also reduces memory consumption and runtime, making our approach more efficient for TTT.

LoRA rank and scale.

As shown in Fig. S5a, increasing the rank does not directly lead to performance gains. Each rank has an optimal scale, and as the rank increases, the corresponding optimal scale tends to decrease. When the rank is small (*e.g.*, rank 4), performance remains stable across different scales, reducing the need for extensive hyperparameter tuning.

LoRA rank and attention matrices.

We investigate the optimal application of LoRA to different attention matrices in CLIP-ViT-B/16. In Fig. S5b, we observe that apply-

Table S6. **Masking strategy.** The LoRA scale γ is set to 2 for both benchmarks. Performance differences from zero-shot CLIP-ViT-B/16 are shown with a blue (\uparrow) or red (\downarrow) arrow.

Reconstruction	Mask Ratio	Cutoff	Decoder	ImageNet	OOD Average	FG Average
Class token	0.25	0.1		67.65 _(\downarrow0.94)	58.94 _(\uparrow1.80)	64.57 _(\downarrow0.92)
	0.5	0.1		67.78 _(\uparrow1.07)	58.85 _(\uparrow1.71)	64.72 _(\uparrow1.08)
	0.75	0.1		67.48 _(\downarrow0.76)	57.87 _(\downarrow0.72)	64.35 _(\downarrow0.71)
	0.5	0.5		67.52 _(\downarrow0.80)	58.30 _(\downarrow1.16)	64.49 _(\downarrow0.84)
	0.5	1		67.20 _(\downarrow0.48)	57.79 _(\downarrow0.65)	64.34 _(\downarrow0.69)
	0.5	0.1	\checkmark	67.27 _(\downarrow0.55)	58.28 _(\uparrow1.14)	64.14 _(\downarrow0.50)
Visual tokens	0.5	0.1		66.89 _(\downarrow0.17)	57.46 _(\downarrow0.32)	63.79 _(\downarrow0.15)
Image pixel	0.5	0.1	\checkmark	66.67 _(\downarrow0.05)	57.05 _(\downarrow0.10)	63.50 _(\downarrow0.14)

ing LoRA to W_v at the same rank achieves the best results among the 4 matrices (W_o , W_v , W_q , and W_k). This trend aligns with previous research [68, 72], even in the context of TTT. Given the same total number of parameters, applying LoRA to W_{kvqo} shows little difference in performance compared to applying it to W_{vq} or W_{kq} .

5.2. Masking strategy

In masked image modeling, the mask strategy plays a crucial role [16, 25]. We examine the effects of the masking ratio, the confidence selection cutoff, the use of an image decoder, and the impact of reconstruction targets. We use a randomly initialized transformer-based decoder with 8 layers, 16 heads, and a 768 embedding size, without prior fine-tuning to ensure a fair evaluation. This decoder allows us to incorporate the pixel-wise reconstruction loss proposed in TTT methods based on MAE [15, 57].

As shown in Tab. S6, while the masking ratio does not significantly affect the overall performance, we choose a default masking ratio of 50% as it strikes a good balance between performance and computational efficiency. As proposed in TPT, selecting and masking the top 10% of augmented images with the lowest entropy yields better performance than masking all 64 images (*i.e.*, applying a cutoff of 1), with an improvement of over 1% observed in the OOD average. The 10% cutoff not only improves performance but also enhances the computational efficiency of TTT by calculating the loss on only one-tenth of the images. Furthermore, reconstructing the class token is more effective than reconstructing masked visual tokens or image pixels using the decoder. This supports the hypothesis that improving zero-shot image classification performance in VLMs relies more on aligning high-level semantics than on capturing fine-grained features.

5.3. Initialization of LoRA weights

LoRA demonstrates high effectiveness and efficiency for TTT, even when initialized with random weights. In this section, we explore the performance gains achieved by fine-tuning the LoRA weights before TTT. We prepare a third dataset, CC3M [46], for LoRA initialization and train only the LoRA weights using the same contrastive loss as in

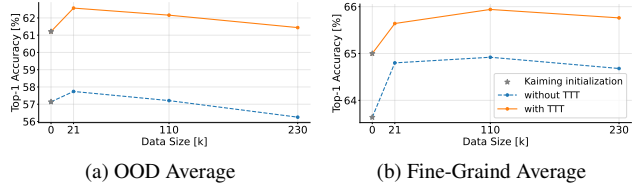


Figure S6. **Impact of LoRA weight initialization** by data size and comparison with TTT.

CLIP pre-training [44] with image-text pairs. We employ Adam with a learning rate of $1e-6$ and a weight decay of 0.05 for optimization, performing one epoch of training with a batch size of 64.

As shown in Fig. S6, LoRA initialization using 21k randomly sampled image-text pairs from CC3M (*i.e.*, only 1% of the total CC3M dataset) improves performance by more than 1% on the fine-grained benchmark and by 0.6% on the OOD benchmark. Furthermore, TTT consistently improves performance on both the benchmarks, regardless of the LoRA initialization. Our experiments demonstrate that fine-tuning LoRA with a small amount of data shows the potential to enhance its performance. While adhering to the constraints of not leveraging domain-specific information or a teacher model, LoRA fine-tuning delivers significant performance improvements in TTT, establishing it as an effective approach for future applications of LoRA in TTT.

6. Conclusion

This paper presents a **Low-Rank Test-Time Training** (LoRA-TTT), a novel test-time training method for VLMs. LoRA-TTT leverages LoRA, enabling effective adaptation to distribution shifts during test time without incurring catastrophic forgetting. Additionally, we introduce a highly efficient reconstruction loss suited for TTT, which enhances the generalization and calibration performance of our method. Extensive experiments on two benchmarks demonstrate that LoRA-TTT outperforms state-of-the-art text prompt tuning methods, while requiring less memory, runtime, and avoiding the need for external resources. These results show that LoRA-TTT can be applied across a wide range of domains and applications, from high-stakes environments to edge devices. We hope our work serves as a foundation for developing new TTT methods for foundation models, unlocking the potential of the image encoder.

References

- [1] Armen Aghajanyan, Luke Zettlemoyer, and Sonal Gupta. Intrinsic dimensionality explains the effectiveness of language model fine-tuning. *arXiv preprint arXiv:2012.13255*, 2020. 3
- [2] Fatemeh Azimi, Sebastian Palacio, Federico Raue, Jörn Hees, Luca Bertinetto, and Andreas Dengel. Self-supervised

- test-time adaptation on video data. In *Proceedings of the IEEE/CVF Winter Conference on Applications of Computer Vision*, pages 3439–3448, 2022. 2, 7
- [3] Lukas Bossard, Matthieu Guillaumin, and Luc Van Gool. Food-101—mining discriminative components with random forests. In *Computer vision—ECCV 2014: 13th European conference, zurich, Switzerland, September 6–12, 2014, proceedings, part VI 13*, pages 446–461. Springer, 2014. 5
- [4] Malik Boudiaf, Romain Mueller, Ismail Ben Ayed, and Luca Bertinetto. Parameter-free online test-time adaptation. In *Proceedings of the IEEE/CVF Conference on Computer Vision and Pattern Recognition*, pages 8344–8353, 2022. 1
- [5] Adrian Bulat and Georgios Tzimiropoulos. Lasp: Text-to-text optimization for language-aware soft prompting of vision & language models. In *Proceedings of the IEEE/CVF Conference on Computer Vision and Pattern Recognition*, pages 23232–23241, 2023. 1
- [6] Han Cai, Chuang Gan, Ligeng Zhu, and Song Han. Tinytl: Reduce memory, not parameters for efficient on-device learning. *Advances in Neural Information Processing Systems*, 33:11285–11297, 2020. 2, 7
- [7] Soravit Changpinyo, Piyush Sharma, Nan Ding, and Radu Soricut. Conceptual 12m: Pushing web-scale image-text pre-training to recognize long-tail visual concepts. In *Proceedings of the IEEE/CVF conference on computer vision and pattern recognition*, pages 3558–3568, 2021. 1
- [8] Dian Chen, Dequan Wang, Trevor Darrell, and Sayna Ebrahimi. Contrastive test-time adaptation. In *Proceedings of the IEEE/CVF Conference on Computer Vision and Pattern Recognition*, pages 295–305, 2022. 1, 2
- [9] Mircea Cimpoi, Subhansu Maji, Iasonas Kokkinos, Sammy Mohamed, and Andrea Vedaldi. Describing textures in the wild. In *Proceedings of the IEEE conference on computer vision and pattern recognition*, pages 3606–3613, 2014. 4
- [10] Jia Deng, Wei Dong, Richard Socher, Li-Jia Li, Kai Li, and Li Fei-Fei. Imagenet: A large-scale hierarchical image database. In *2009 IEEE conference on computer vision and pattern recognition*, pages 248–255. Ieee, 2009. 4
- [11] Ning Ding, Yujia Qin, Guang Yang, Fuchao Wei, Zonghan Yang, Yusheng Su, Shengding Hu, Yulin Chen, Chi-Min Chan, Weize Chen, et al. Parameter-efficient fine-tuning of large-scale pre-trained language models. *Nature Machine Intelligence*, 5(3):220–235, 2023. 2
- [12] Vishnu Sashank Dorbala, Gunnar Sigurdsson, Robinson Piramuthu, Jesse Thomason, and Gaurav S Sukhatme. Clipnav: Using clip for zero-shot vision-and-language navigation. *arXiv preprint arXiv:2211.16649*, 2022. 2, 6, 7
- [13] Matteo Farina, Gianni Franchi, Giovanni Iacca, Massimiliano Mancini, and Elisa Ricci. Frustratingly easy test-time adaptation of vision-language models. *arXiv preprint arXiv:2405.18330*, 2024. 3
- [14] Chun-Mei Feng, Kai Yu, Yong Liu, Salman Khan, and Wangmeng Zuo. Diverse data augmentation with diffusions for effective test-time prompt tuning. In *Proceedings of the IEEE/CVF International Conference on Computer Vision*, pages 2704–2714, 2023. 2, 4
- [15] Yossi Gandelsman, Yu Sun, Xinlei Chen, and Alexei Efros. Test-time training with masked autoencoders. *Advances in Neural Information Processing Systems*, 35:29374–29385, 2022. 2, 4, 8
- [16] Peng Gao, Ziyi Lin, Renrui Zhang, Rongyao Fang, Hongyang Li, Hongsheng Li, and Yu Qiao. Mimic before reconstruct: Enhancing masked autoencoders with feature mimicking. *International Journal of Computer Vision*, 132(5):1546–1556, 2024. 8
- [17] Jindong Gu, Zhen Han, Shuo Chen, Ahmad Beirami, Bailan He, Gengyuan Zhang, Ruotong Liao, Yao Qin, Volker Tresp, and Philip Torr. A systematic survey of prompt engineering on vision-language foundation models. *arXiv preprint arXiv:2307.12980*, 2023. 1, 6
- [18] Chuan Guo, Geoff Pleiss, Yu Sun, and Kilian Q Weinberger. On calibration of modern neural networks. In *International conference on machine learning*, pages 1321–1330. PMLR, 2017. 2, 6
- [19] Zeyu Han, Chao Gao, Jinyang Liu, Sai Qian Zhang, et al. Parameter-efficient fine-tuning for large models: A comprehensive survey. *arXiv preprint arXiv:2403.14608*, 2024. 2, 3
- [20] Kaiming He, Xiangyu Zhang, Shaoqing Ren, and Jian Sun. Delving deep into rectifiers: Surpassing human-level performance on imagenet classification. In *Proceedings of the IEEE international conference on computer vision*, pages 1026–1034, 2015. 5
- [21] Kaiming He, Xinlei Chen, Saining Xie, Yanghao Li, Piotr Dollár, and Ross Girshick. Masked autoencoders are scalable vision learners. In *Proceedings of the IEEE/CVF conference on computer vision and pattern recognition*, pages 16000–16009, 2022. 4
- [22] Patrick Helber, Benjamin Bischke, Andreas Dengel, and Damian Borth. Eurosat: A novel dataset and deep learning benchmark for land use and land cover classification. *IEEE Journal of Selected Topics in Applied Earth Observations and Remote Sensing*, 12(7):2217–2226, 2019. 5
- [23] Dan Hendrycks, Steven Basart, Norman Mu, Saurav Kadavath, Frank Wang, Evan Dorundo, Rahul Desai, Tyler Zhu, Samyak Parajuli, Mike Guo, et al. The many faces of robustness: A critical analysis of out-of-distribution generalization. In *Proceedings of the IEEE/CVF international conference on computer vision*, pages 8340–8349, 2021. 4
- [24] Dan Hendrycks, Kevin Zhao, Steven Basart, Jacob Steinhardt, and Dawn Song. Natural adversarial examples. In *Proceedings of the IEEE/CVF conference on computer vision and pattern recognition*, pages 15262–15271, 2021. 4
- [25] Vlad Hondru, Florinel Alin Croitoru, Shervin Minaee, Radu Tudor Ionescu, and Nicu Sebe. Masked image modeling: A survey. *arXiv preprint arXiv:2408.06687*, 2024. 8
- [26] Edward J Hu, Yelong Shen, Phillip Wallis, Zeyuan Allen-Zhu, Yuanzhi Li, Shean Wang, Lu Wang, and Weizhu Chen. Lora: Low-rank adaptation of large language models. *arXiv preprint arXiv:2106.09685*, 2021. 2, 3
- [27] Chao Jia, Yinfei Yang, Ye Xia, Yi-Ting Chen, Zarana Parekh, Hieu Pham, Quoc Le, Yun-Hsuan Sung, Zhen Li, and Tom Duerig. Scaling up visual and vision-language representation learning with noisy text supervision. In *International conference on machine learning*, pages 4904–4916. PMLR, 2021. 1

- [28] Adilbek Karmanov, Dayan Guan, Shijian Lu, Abdulmotaleb El Saddik, and Eric Xing. Efficient test-time adaptation of vision-language models. In *Proceedings of the IEEE/CVF Conference on Computer Vision and Pattern Recognition*, pages 14162–14171, 2024. 2, 4
- [29] Apoorv Khandelwal, Luca Weihs, Roozbeh Mottaghi, and Aniruddha Kembhavi. Simple but effective: Clip embeddings for embodied ai. In *Proceedings of the IEEE/CVF Conference on Computer Vision and Pattern Recognition*, pages 14829–14838, 2022. 2, 6, 7
- [30] Jonathan Krause, Michael Stark, Jia Deng, and Li Fei-Fei. 3d object representations for fine-grained categorization. In *Proceedings of the IEEE international conference on computer vision workshops*, pages 554–561, 2013. 5
- [31] Ananya Kumar, Aditi Raghunathan, Robbie Jones, Tengyu Ma, and Percy Liang. Fine-tuning can distort pretrained features and underperform out-of-distribution. *arXiv preprint arXiv:2202.10054*, 2022. 2, 3
- [32] Boyi Li, Kilian Q Weinberger, Serge Belongie, Vladlen Koltun, and René Ranftl. Language-driven semantic segmentation. *arXiv preprint arXiv:2201.03546*, 2022. 3
- [33] Fei-Fei Li, Marco Andreoto, M Ranzato, and Pietro Perona. Caltech 101. *CaltechDATA: Pasadena, CA, USA*, 2022. 5
- [34] Jian Liang, Ran He, and Tieniu Tan. A comprehensive survey on test-time adaptation under distribution shifts. *International Journal of Computer Vision*, pages 1–34, 2024. 2
- [35] Jie Liu, Yixiao Zhang, Jie-Neng Chen, Junfei Xiao, Yongyi Lu, Bennett A Landman, Yixuan Yuan, Alan Yuille, Yucheng Tang, and Zongwei Zhou. Clip-driven universal model for organ segmentation and tumor detection. In *Proceedings of the IEEE/CVF International Conference on Computer Vision*, pages 21152–21164, 2023. 2, 6, 7
- [36] Jiaming Liu, Ran Xu, Senqiao Yang, Renrui Zhang, Qizhe Zhang, Zehui Chen, Yandong Guo, and Shanghang Zhang. Continual-mae: Adaptive distribution masked autoencoders for continual test-time adaptation. In *Proceedings of the IEEE/CVF Conference on Computer Vision and Pattern Recognition*, pages 28653–28663, 2024. 2
- [37] Ilya Loshchilov and Frank Hutter. Decoupled weight decay regularization. *arXiv preprint arXiv:1711.05101*, 2017. 5
- [38] Subhransu Maji, Esa Rahtu, Juho Kannala, Matthew Blaschko, and Andrea Vedaldi. Fine-grained visual classification of aircraft. *arXiv preprint arXiv:1306.5151*, 2013. 5
- [39] Jan Hendrik Metzen, Piyapat Saranrittichai, and Chaithanya Kumar Mummadi. Autoclip: Auto-tuning zero-shot classifiers for vision-language models. *arXiv preprint arXiv:2309.16414*, 2023. 1
- [40] Matthias Minderer, Alexey Gritsenko, Austin Stone, Maxim Neumann, Dirk Weissenborn, Alexey Dosovitskiy, Aravindh Mahendran, Anurag Arnab, Mostafa Dehghani, Zhuoran Shen, et al. Simple open-vocabulary object detection. In *European Conference on Computer Vision*, pages 728–755. Springer, 2022. 3
- [41] Mahdi Pakdaman Naeini, Gregory Cooper, and Milos Hauskrecht. Obtaining well calibrated probabilities using bayesian binning. In *Proceedings of the AAAI conference on artificial intelligence*, 2015. 6
- [42] Maria-Elena Nilsback and Andrew Zisserman. Automated flower classification over a large number of classes. In *2008 Sixth Indian conference on computer vision, graphics & image processing*, pages 722–729. IEEE, 2008. 4
- [43] Omkar M Parkhi, Andrea Vedaldi, Andrew Zisserman, and CV Jawahar. Cats and dogs. In *2012 IEEE conference on computer vision and pattern recognition*, pages 3498–3505. IEEE, 2012. 4
- [44] Alec Radford, Jong Wook Kim, Chris Hallacy, Aditya Ramesh, Gabriel Goh, Sandhini Agarwal, Girish Sastry, Amanda Askell, Pamela Mishkin, Jack Clark, et al. Learning transferable visual models from natural language supervision. In *International conference on machine learning*, pages 8748–8763. PMLR, 2021. 1, 3, 5, 8
- [45] Benjamin Recht, Rebecca Roelofs, Ludwig Schmidt, and Vaishal Shankar. Do imagenet classifiers generalize to imagenet? In *International conference on machine learning*, pages 5389–5400. PMLR, 2019. 4
- [46] Piyush Sharma, Nan Ding, Sebastian Goodman, and Radu Soricut. Conceptual captions: A cleaned, hypernymed, image alt-text dataset for automatic image captioning. In *Proceedings of the 56th Annual Meeting of the Association for Computational Linguistics (Volume 1: Long Papers)*, pages 2556–2565, 2018. 1, 8
- [47] Manli Shu, Weili Nie, De-An Huang, Zhiding Yu, Tom Goldstein, Anima Anandkumar, and Chaowei Xiao. Test-time prompt tuning for zero-shot generalization in vision-language models. *Advances in Neural Information Processing Systems*, 35:14274–14289, 2022. 1, 2, 3, 4, 5, 6
- [48] Yang Shu, Xingzhuo Guo, Jialong Wu, Ximei Wang, Jianmin Wang, and Mingsheng Long. Clipood: Generalizing clip to out-of-distributions. In *International Conference on Machine Learning*, pages 31716–31731. PMLR, 2023. 1
- [49] Junha Song, Jungsoo Lee, In So Kweon, and Sungha Choi. Ecotta: Memory-efficient continual test-time adaptation via self-distilled regularization. In *Proceedings of the IEEE/CVF Conference on Computer Vision and Pattern Recognition*, pages 11920–11929, 2023. 2, 7
- [50] Khurram Soomro, Amir Roshan Zamir, and Mubarak Shah. Ucf101: A dataset of 101 human actions classes from videos in the wild. *arXiv preprint arXiv:1212.0402*, 2012. 5
- [51] Elaine Sui, Xiaohan Wang, and Serena Yeung-Levy. Just shift it: Test-time prototype shifting for zero-shot generalization with vision-language models. *arXiv preprint arXiv:2403.12952*, 2024. 1
- [52] Yu Sun, Xiaolong Wang, Zhuang Liu, John Miller, Alexei Efros, and Moritz Hardt. Test-time training with self-supervision for generalization under distribution shifts. In *International conference on machine learning*, pages 9229–9248. PMLR, 2020. 2
- [53] Bart Thomee, David A Shamma, Gerald Friedland, Benjamin Elizalde, Karl Ni, Douglas Poland, Damian Borth, and Li-Jia Li. Yfcc100m: The new data in multimedia research. *Communications of the ACM*, 59(2):64–73, 2016. 1
- [54] Dequan Wang, Evan Shelhamer, Shaoteng Liu, Bruno Olshausen, and Trevor Darrell. Tent: Fully test-time adaptation by entropy minimization. *arXiv preprint arXiv:2006.10726*, 2020. 1, 2, 4

- [55] Haohan Wang, Songwei Ge, Zachary Lipton, and Eric P King. Learning robust global representations by penalizing local predictive power. *Advances in Neural Information Processing Systems*, 32, 2019. 4
- [56] Mengmeng Wang, Jiazheng Xing, and Yong Liu. Actionclip: A new paradigm for video action recognition. *arXiv preprint arXiv:2109.08472*, 2021. 3
- [57] Renhao Wang, Yu Sun, Yossi Gandelsman, Xinlei Chen, Alexei A Efros, and Xiaolong Wang. Test-time training on video streams. *arXiv preprint arXiv:2307.05014*, 2023. 2, 4, 7, 8
- [58] Zifeng Wang, Zhenbang Wu, Dinesh Agarwal, and Jimeng Sun. Medclip: Contrastive learning from unpaired medical images and text. *arXiv preprint arXiv:2210.10163*, 2022. 2, 6, 7
- [59] Zixin Wang, Yadan Luo, Liang Zheng, Zhuoxiao Chen, Sen Wang, and Zi Huang. In search of lost online test-time adaptation: A survey. *International Journal of Computer Vision*, pages 1–34, 2024. 2
- [60] Mitchell Wortsman, Gabriel Ilharco, Jong Wook Kim, Mike Li, Simon Kornblith, Rebecca Roelofs, Raphael Gontijo Lopes, Hannaneh Hajishirzi, Ali Farhadi, Hongseok Namkoong, et al. Robust fine-tuning of zero-shot models. In *Proceedings of the IEEE/CVF conference on computer vision and pattern recognition*, pages 7959–7971, 2022. 2, 3
- [61] Jianxiong Xiao, James Hays, Krista A Ehinger, Aude Oliva, and Antonio Torralba. Sun database: Large-scale scene recognition from abbey to zoo. In *2010 IEEE computer society conference on computer vision and pattern recognition*, pages 3485–3492. IEEE, 2010. 4
- [62] Zehao Xiao, Jiayi Shen, Mohammad Mahdi Derakhshani, Shengcai Liao, and Cees GM Snoek. Any-shift prompting for generalization over distributions. In *Proceedings of the IEEE/CVF Conference on Computer Vision and Pattern Recognition*, pages 13849–13860, 2024. 1
- [63] Yi Xin, Siqi Luo, Haodi Zhou, Junlong Du, Xiaohong Liu, Yue Fan, Qing Li, and Yuntao Du. Parameter-efficient fine-tuning for pre-trained vision models: A survey. *arXiv preprint arXiv:2402.02242*, 2024. 3
- [64] Lingling Xu, Haoran Xie, Si-Zhao Joe Qin, Xiaohui Tao, and Fu Lee Wang. Parameter-efficient fine-tuning methods for pretrained language models: A critical review and assessment. *arXiv preprint arXiv:2312.12148*, 2023. 2
- [65] Lewei Yao, Runhui Huang, Lu Hou, Guansong Lu, Minzhe Niu, Hang Xu, Xiaodan Liang, Zhenguo Li, Xin Jiang, and Chunjing Xu. Filip: Fine-grained interactive language-image pre-training. *arXiv preprint arXiv:2111.07783*, 2021. 3
- [66] Hee Suk Yoon, Eunseop Yoon, Joshua Tian Jin Tee, Mark Hasegawa-Johnson, Yingzhen Li, and Chang D Yoo. C-tp: Calibrated test-time prompt tuning for vision-language models via text feature dispersion. *arXiv preprint arXiv:2403.14119*, 2024. 1, 2, 5, 6
- [67] Jiahui Yu, Zirui Wang, Vijay Vasudevan, Legg Yeung, Mojtaba Seyedhosseini, and Yonghui Wu. Coca: Contrastive captioners are image-text foundation models. *arXiv preprint arXiv:2205.01917*, 2022. 3
- [68] Maxime Zanella and Ismail Ben Ayed. Low-rank few-shot adaptation of vision-language models. In *Proceedings of the IEEE/CVF Conference on Computer Vision and Pattern Recognition*, pages 1593–1603, 2024. 3, 8
- [69] Maxime Zanella and Ismail Ben Ayed. On the test-time zero-shot generalization of vision-language models: Do we really need prompt learning? In *Proceedings of the IEEE/CVF Conference on Computer Vision and Pattern Recognition*, pages 23783–23793, 2024. 2, 5, 6
- [70] Jingyi Zhang, Jiaxing Huang, Sheng Jin, and Shijian Lu. Vision-language models for vision tasks: A survey. *IEEE Transactions on Pattern Analysis and Machine Intelligence*, 2024. 2
- [71] Marvin Zhang, Sergey Levine, and Chelsea Finn. Memo: Test time robustness via adaptation and augmentation. *Advances in neural information processing systems*, 35:38629–38642, 2022. 2, 3
- [72] Qingru Zhang, Minshuo Chen, Alexander Bukharin, Nikos Karampatziakis, Pengcheng He, Yu Cheng, Weizhu Chen, and Tuo Zhao. Adalora: Adaptive budget allocation for parameter-efficient fine-tuning. *arXiv preprint arXiv:2303.10512*, 2023. 7, 8
- [73] Shuai Zhao, Xiaohan Wang, Linchao Zhu, and Yi Yang. Test-time adaptation with clip reward for zero-shot generalization in vision-language models. *arXiv preprint arXiv:2305.18010*, 2023. 2, 4
- [74] Kaiyang Zhou, Jingkang Yang, Chen Change Loy, and Ziwei Liu. Conditional prompt learning for vision-language models. In *Proceedings of the IEEE/CVF conference on computer vision and pattern recognition*, pages 16816–16825, 2022. 1, 5, 6
- [75] Kaiyang Zhou, Jingkang Yang, Chen Change Loy, and Ziwei Liu. Learning to prompt for vision-language models. *International Journal of Computer Vision*, 130(9):2337–2348, 2022. 1, 5, 6
- [76] Beier Zhu, Yulei Niu, Yucheng Han, Yue Wu, and Hanwang Zhang. Prompt-aligned gradient for prompt tuning. In *Proceedings of the IEEE/CVF International Conference on Computer Vision*, pages 15659–15669, 2023. 1
- [77] Yitao Zhu, Zhenrong Shen, Zihao Zhao, Sheng Wang, Xin Wang, Xiangyu Zhao, Dinggang Shen, and Qian Wang. Melo: Low-rank adaptation is better than fine-tuning for medical image diagnosis. In *2024 IEEE International Symposium on Biomedical Imaging (ISBI)*, pages 1–5. IEEE, 2024. 3